

Specific Heat Capacity at Constant Volume for Water, Methanol, and Their Mixtures at Temperatures from 300 K to 400 K and Pressures to 20 MPa[†]

Takahiro Kuroki, Noboru Kagawa,* Harumi Endo, Seizou Tsuruno, and Joseph W. Magee[‡]

National Defense Academy, Yokosuka 239-0811, Japan

Specific heat capacities at constant volume (c_v) of water, methanol, and their mixtures were measured with a new adiabatic calorimeter. Temperatures ranged from 300 K to 400 K, and pressures ranged to 20 MPa. Densities were determined at the initial and final end points during each calorimetric experiment. The calorimeter is a twin-cell type whose sample and reference cells (33 cm³) and their shields are heated by electric power. The cells are surrounded by a high vacuum. During the experiment, the heating power was carefully controlled so that the cell temperature increased uniformly. The reference cell was always evacuated and was heated with a constant current. The temperature of the sample cell tracked that of the reference cell temperature by means an automatic control system. Automated sample pressure measurements were made with a crystal quartz transducer. The expanded relative uncertainty for c_v is estimated to be 1% for liquid-phase measurements, and for density it is about 0.2%.

Introduction

To develop a reliable equation of state for a fluid, various thermodynamic property measurements of the fluid are required. Among them, isochoric heat capacity measurements provide a very useful check for calculations of the second derivative of the pressure with respect to temperature, which is essential information to develop an accurate equation but is challenging to measure accurately. By use of molecular theory, vibrational and orientational modes of molecules can account for the thermodynamic properties of a substance. When a substance is heated, the increasing vibrational energy stored in molecules makes a strong contribution to the heat capacity. On the other hand, changes of molecular structure with temperature can also affect the magnitude of the heat capacity contribution which is dominated by orientational energy.

Hydrogen bonding of water (H₂O) is certain to introduce the effect of the molecular energy to the heat capacity. In fact, interactions between water and methanol (CH₃OH) molecules show anomalous thermodynamic properties due to the presence of strong hydrogen bonding.¹ There has been, even very recently, considerable interest in the physical property behavior of H₂O + CH₃OH mixtures in the supercritical and high-density regions; for example, *PVTx* properties,^{2–4} excess molar heat capacity, and excess molar enthalpies^{5–7} have been reported. However, published information on the isochoric heat capacity of the mixtures is limited to recent work by Abdulgatov et al.,⁸ who reported isochoric heat capacities for an equimass H₂O + CH₃OH mixture in a range of temperatures from 435 K

to 645 K. To better characterize the H₂O + CH₃OH system, additional measurements are needed that cover a wide range of temperatures, pressures, and compositions.

To measure the heat capacity of fluids, various methods have been proposed;⁹ however, the high accuracy potential of adiabatic methods makes them the most desirable. In the adiabatic principle, heat exchange between the calorimeter and the surroundings does not occur in the system; thus, the energy applied to the sample cell would be precisely the desired quantity to calculate the heat flow and heat capacity. In actual practice, however, the ideal adiabatic condition is very difficult to realize due to heat leakage by thermal conduction, convection, and thermal radiation. If the heat leakage is considerable, it may be important to evaluate the amount of the heat leakage accurately to correct the measured values. A small heat leak is self-correcting if we use the twin calorimeter method in which there are two identical vessels (cells) in identical surroundings. In one cell is the sample to be measured, and in the other either there is a reference fluid or it may be empty. A novel twin-cell adiabatic calorimeter^{10,11} has been developed in the NIST labs; it has been applied to measure H₂O and H₂O + NH₃ mixtures.^{11,12} In a recent development, a new twin-cell adiabatic calorimeter¹³ was built in Japan which traces its roots to the design of the NIST calorimeter but features numerous improvements such as a smaller size and greater simplicity in its design.

In this paper, we report the first measurements with this new calorimeter. Water was chosen for apparatus validation due to its well-established thermodynamic surface. Methanol and methanol + water mixtures were selected to establish the performance of the calorimeter for a mixture system of scientific and industrial interest. We will report heat capacities of H₂O, CH₃OH, and their mixtures for liquid samples in a range of temperatures from 280 K to 400 K. In addition, we will report density values that were calculated from the volume of the calorimeter cell and sample mass measurements.

[†] This contribution will be part of a special print edition containing papers presented at the Fourteenth Symposium on Thermophysical Properties, Boulder, CO, June 25–30, 2000.

* To whom correspondence should be addressed. E-mail: kagawa@nda.ac.jp. Fax: +81-468-44-5900.

[‡] Permanent address: Physical and Chemical Properties Division, National Institute of Standards and Technology, Boulder, CO 80305-3328.

Table 1. Mass Fraction w and Mole Fraction x of $\{x\text{H}_2\text{O} + (1-x)\text{CH}_3\text{OH}\}$ Mixtures Used in This Study

w	x
0.19010	0.29452
0.64858	0.76649

Experimental Section

Materials. High-purity samples of H_2O and CH_3OH were obtained to prepare the mixtures. The H_2O sample was twice-distilled and has a minimum purity of 0.9999 mass fraction and an insulating resistance of $18 \text{ M}\Omega \cdot \text{cm}$. For the CH_3OH sample, the commercial supplier claimed a minimum liquid purity of 0.998 mass fraction with 0.001 mass fraction H_2O and 0.0005 mass fraction $\text{C}_2\text{H}_5\text{OH}$. Each component was degassed twice and was stored in a lightweight cylinder (75 cm^3). The sample cylinders were accurately weighed with a 0.1 mg uncertainty.

The mixtures were prepared in the calorimeter cell by introducing each component through evacuated tubing. During the transfer step, each component was heated above 373 K to enable faster transfer. After both components of the mixture were charged from the cylinders into the calorimeter cell, the cell was cooled below 278 K by a minicooler. The remaining mass in each cylinder was weighed and then the composition of the sample in the cell was calculated from the masses charged to the cell. To ensure complete homogenization, the sample cell temperature was increased until the sample pressure reached the apparatus pressure limit of 20 MPa. This process was carried out twice before the first measurement was begun. Both the mass fraction and mole fraction compositions of the two mixtures prepared for this study are given in Table 1. The expanded uncertainty (coverage factor $k = 2$) of the mass fraction composition is 0.002, after including the uncertainty due to the impurities of the constituents.

Measurements. The twin-cell adiabatic calorimeter,¹³ shown in Figure 1, was used for these measurements. A type-304 stainless steel spherical cell of 33 cm^3 capacity was designed for this apparatus. It has a maximum permissible pressure of 60 MPa at 800 K. A pair of these cells was made from stainless steel block by spinning in a lathe within a $\pm 5 \mu\text{m}$ tolerance to produce hemispheres which then were welded together. On the bottom of each cell was brazed a copper block to accept a platinum resistance thermometer (PRT). Absolute temperatures are measured with the PRT's and are reported on the ITS-90. Sheath heaters, which were specially insulated and are capable of reaching 900 K in a vacuum were prepared for this apparatus. A 2Ω heater was wound around each sphere with a pitch of about 8 mm. Small strips were attached to the cell surface to hold the heater wires in place.

A 6.4 mm outer diameter (o.d.) type-316 stainless steel tube was welded into a hole in the top of each sphere. A 1.735 mm inner diameter capillary was welded into the 6.4 mm o.d. tube. Two type-K thermocouples sealed in a stainless steel sheath were put on each cell surface to read the temperature difference between each cell and its associated adiabatic shield, also made from type-304 stainless steel. Each spherical cell was jacketed in a cylindrical adiabatic shield whose temperature was adjusted by a 3Ω sheath heater for the sides and a 0.8Ω one for the top to keep it in equilibrium with the cell temperature. To control the temperature, two type-K thermocouples were put onto the surface of each adiabatic shield side and one was put onto each shield top. A pressure transducer using a precision quartz-crystal resonator, attached to the charg-

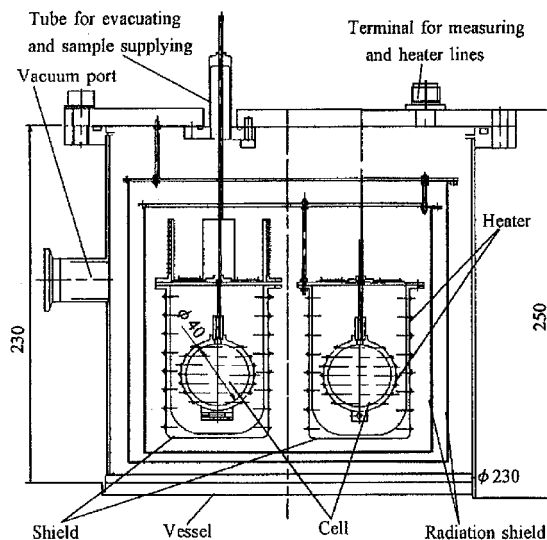


Figure 1. Twin-cell adiabatic calorimeter.

ing manifold, provided pressure measurements to 68 MPa. Adiabatic conditions are ensured by each thermal radiation shield and by maintaining a high vacuum (approximately $1 \times 10^{-4} \text{ Pa}$) in the vacuum vessel that surrounds both cell/adiabatic shield assemblies.

Each of the six heaters (cell, shield side, and shield top for each set) in the calorimeter was driven by a direct-current power supply system. Two 4-channel 16-bit A/D converters control it. The entire instrument was connected to a personal computer through an IEEE-488 standard interface bus. The computer carried out several functions of temperature control and data acquisition with the aid of a graphical programming language and a specialized program. The measurement and temperature-control tasks were executed every 30 s during the course of an experiment. Between measurement cycles, the cell temperature rose about 35 mK. The temperature difference between the cells was maintained within $\pm 3 \text{ mK}$ during a measurement. In addition, the system controlled each temperature difference between the cells and shield sides, and between the cells and shield tops, within $\pm 10 \text{ mK}$.

For the heat capacity measurement, a precisely determined electrical energy (Q) is applied and the resulting temperature rise ($\Delta T = T_2 - T_1$) is measured. The isochoric specific heat capacity is obtained from

$$c_v = \left(\frac{\partial U}{\partial T} \right)_V \cong \frac{\Delta Q - \Delta Q_0 - \Delta W_{PV}}{m\Delta T} \quad (1)$$

where U is the internal energy, ΔQ_0 is the energy difference between the sample cell, $Q_{0,\text{sam}}$, and the reference cell, $Q_{0,\text{ref}}$, when the cells are empty, ΔQ refers to the energy added during an experiment with a sample in the sample cell and a blank (vacuum) in the reference cell, W_{PV} is the change-of-volume work due to the slight dilation of the cell, and m is the mass of sample in the sample cell.

To prepare for measurements, the sample cell was charged with the sample and was cooled to a starting temperature below room temperature. Then, measurements were performed by raising the temperature until the upper pressure limit of 20 MPa was reached. At the completion of a run, a portion of the sample in the cell was cryopumped into a lightweight cylinder and was weighed. The next run was started with a lower density. When the runs were completed, the remaining sample in the cell was

Table 2. Expanded Uncertainties for This Work

temperature	
absolute	0.04 K
difference, ΔT	0.0011 K
pressure	0.007 MPa
mass	0.0002 g
volume	0.007 cm ³
composition, mass fraction	0.002
density	0.2%
energy	
power	0.02%
difference	0.25 J
change-of-volume work	2%
specific heat capacity	1%

discharged and weighed. The sample mass of each run was determined from the sum of the appropriate mass increments for that run.

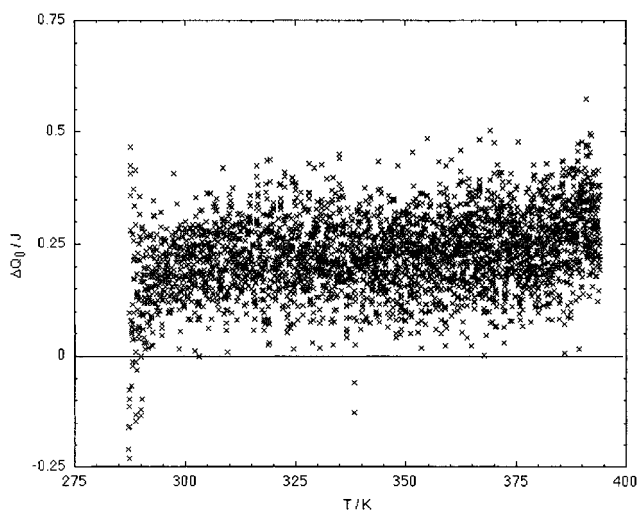
Uncertainties. In the following discussion, a definition is used for the expanded uncertainty that is two times the standard uncertainty (a coverage factor $k = 2$). The estimated uncertainty of the absolute temperature measurement based on ITS-90 is ± 40 mK, even though the stability of the PRT readings was ± 2.5 mK. It was obtained by considering the temperature distribution on the cell (± 10 mK to 20 mK) and the systematic accuracy of the instruments (± 4 mK). The temperature distribution on the cell was measured with the two thermocouples placed on the top and bottom sides of each cell. The uncertainty of the temperature rise at the experimental ramp rate of $+70$ mK \cdot min⁻¹ is ± 1.1 mK obtained from the 0.8 mK standard uncertainty of the experimental temperatures from the temperature ramp curve. The uncertainty of the pressure measurement is ± 7 kPa, on the basis of the pressure transducer's specifications. However, the uncertainty deteriorates exponentially at pressures below 10% of the full scale of 68 MPa. To improve the uncertainty, another pressure transducer with a lower full scale will be prepared for lower pressure measurements. The uncertainty of the change-of-volume work, which was calculated¹⁴ with eq 2 below, may be determined from experimental *PVT* data because the derivative of the pressure with respect to temperature could be estimated from the measured temperature rise and pressure difference.

$$W_{PV} = \left(T_2 \left(\frac{\partial P}{\partial T} \right)_{V_2} - \frac{1}{2} \Delta P \right) \Delta V \quad (2)$$

From the fluctuation of the experimental data, the estimated uncertainty of the change-of-volume work is $\pm 2\%$, which leads to an uncertainty in specific heat capacity of $\pm 0.08\%$.

The energy applied to the cells is the product of the constant power and the time interval to heat from T_1 to T_2 . The measurements of the electrical quantities are exceptionally accurate and have an estimated uncertainty of $\pm 0.02\%$. A function of temperature was fitted to the energy difference ΔQ_0 applied to the empty cells; its fluctuation is less than ± 2.5 J \cdot K⁻¹, which propagates an added uncertainty of $\pm 0.5\%$ to the specific heat capacity. By combining the various sources of experimental uncertainty, the expanded uncertainty of the specific heat capacity is estimated to be $\pm 1\%$. The expanded uncertainties and the resulting combined uncertainties are shown in Table 2.

Blank Tests. The empty calorimeter energy function was determined from heating the evacuated cells. Heating experiments covering a temperature range from 280 K to 400 K were repeated before each series. The energy data in unit of joules are shown in Figure 2. An equation for

**Figure 2.** Measured ΔQ_0 as a function of temperature.

the temperature was fit to the data; most data agreed with eq 3 within ± 0.25 J.

$$\Delta Q_0 = [(8.6260 \times 10^{-4}) \text{ J}\cdot\text{K}^{-1}]T - 0.070299 \text{ J} \quad (3)$$

Heat Capacity and Density Results

The isochoric specific heat capacity data c_v of each run is shown in Table 3. Each density ρ was calculated from the measured sample mass and the calibrated cell volume at the measured temperature and pressure. As shown in eq 4, the calibrated cell volume V_{cell} in cubic centimeters is obtained from the coefficient of thermal expansion of stainless steel and a coefficient related to the pressure-dependence of the volume derived from the experimental data.

$$V_{\text{cell}} = \{0.00153 \text{ cm}^3\cdot\text{K}^{-1}(T - 273.15 \text{ K}) + 33.132 \text{ cm}^3\} (1 + (4.40 \times 10^{-5} \text{ MPa}^{-1})P) \quad (4)$$

The coefficient of thermal expansion of type-304 stainless steel was obtained from a handbook¹⁵ and has a claimed uncertainty of 10^{-5} cm³ \cdot K⁻¹. The coefficient of pressure dilation of the sample cell was determined from the slope of the experimental isochore of water with an uncertainty of 4×10^{-6} MPa⁻¹. The reliability of the coefficient was confirmed with a numerical stress analysis for the cell. The uncertainty of the cell volume is estimated to be 0.007 cm³.

A portion of the sample mass resides in the noxious volume that consists of the combined volumes of the connecting tubing, the charging valve orifices, and the pressure transducer. In total, the noxious volume is approximately 3% of the cell volume; as much as 0.8 g of sample could reside in the noxious volume at the maximum density of the measurements. The amount of sample mass in the noxious volume was calculated from an assumed temperature profile of this volume and from densities calculated with an equation of state¹⁶ or correlations based on measured *PVTx* information from this apparatus. To estimate the temperature profile, the volume was divided into five sections: four along the 1.735 mm inner diameter capillary and one for the rest of the noxious volume. At one end, the temperature was measured with a thermometer located inside the pressure transducer. The other was assumed to be at the calorimeter cell temperature. It was assumed that the expanded uncertainty of the noxious volume is about 0.08 cm³. Although the uncertainty of the

Table 3. Experimental Densities and Heat Capacities for H₂O, CH₃OH, 0.29452 H₂O + 0.70548 CH₃OH, and 0.76649 H₂O + 0.23351 CH₃OH

T_1^a	P^b	ρ^c	c_v^d	T_1^a	P^b	ρ^c	c_v^d	T_1^a	P^b	ρ^c	c_v^d	T_1^a	P^b	ρ^c	c_v^d
H ₂ O															
316.177	2.200	991.82	4.078	325.180	9.219	991.05	4.011	334.168	17.709	990.22	3.916	358.173	9.925	972.97	3.824
317.164	2.825	991.74	4.003	326.154	10.082	990.96	4.009	335.175	18.722	990.12	3.910	359.155	11.117	972.87	3.828
318.161	3.524	991.66	4.073	327.164	10.996	990.87	3.992	336.181	19.741	990.03	3.879	360.165	12.353	972.76	3.811
319.171	4.267	991.57	4.041	328.162	11.911	990.78	3.983	337.173	4.082	973.48	3.864	361.171	13.589	972.66	3.830
320.186	5.053	991.49	4.035	329.153	12.840	990.69	3.951	338.173	5.181	973.39	3.861	362.170	14.830	972.55	3.805
321.181	5.841	991.40	3.992	330.180	13.812	990.59	3.969	339.173	6.334	973.28	3.842	363.155	16.068	972.45	3.769
322.163	6.647	991.32	4.002	331.169	14.759	990.50	3.939	339.173	7.530	973.18	3.827	364.175	17.342	972.34	3.828
323.186	7.498	991.23	4.020	332.151	15.714	990.41	3.957	339.173	8.699	973.08	3.856	365.158	18.588	972.24	3.787
324.170	8.337	991.14	3.991	333.169	16.711	990.31	3.916								
CH ₃ OH															
285.153	0.943	798.54		306.154	18.754	796.95	2.213	333.171	0.347	752.94	2.380	353.161	15.373	751.53	2.514
286.172	1.924	798.45		307.151	19.571	796.88	2.234	334.177	1.091	752.87	2.391	354.171	16.139	751.46	2.508
287.179	2.830	798.37		313.150	4.643	776.83		335.159	1.821	752.79	2.423	355.178	16.901	751.39	2.510
288.163	3.711	798.29		314.150	5.502	776.75		336.170	2.581	752.71	2.416	356.154	17.635	751.33	2.487
289.177	4.610	798.21		315.178	6.366	776.68		337.180	3.336	752.64	2.406	357.151	18.387	751.26	2.502
290.195	5.492	798.13		316.184	7.216	776.60		338.180	4.088	752.57	2.408	358.170	19.160	751.19	2.525
291.150	6.321	798.06		317.185	8.063	776.52		339.174	4.835	752.50	2.417	359.154	19.910	751.13	2.500
292.158	7.186	797.98		318.183	8.908	776.45	2.281	340.167	5.580	752.43	2.427	378.155	1.119	705.94	2.690
293.161	8.032	797.91		319.172	9.743	776.37	2.302	341.154	6.321	752.36	2.442	379.153	1.625	705.89	2.715
294.162	8.866	797.84	2.139	320.157	10.571	776.30	2.312	342.169	7.085	752.29	2.460	380.171	2.178	705.83	2.713
295.158	9.693	797.76	2.134	321.174	11.420	776.22	2.325	343.182	7.849	752.22	2.450	381.158	2.810	705.77	2.692
296.150	10.510	797.69	2.148	322.151	12.233	776.15	2.308	344.155	8.584	752.15	2.455	382.161	3.460	705.71	2.691
297.185	11.364	797.61	2.167	323.157	13.066	776.08	2.297	345.157	9.338	752.08	2.437	383.153	4.106	705.65	2.707
298.182	12.170	797.54	2.154	324.161	13.893	776.00	2.317	346.181	10.108	752.01	2.449	384.165	4.765	705.58	2.714
299.208	13.013	797.47	2.186	325.160	14.719	775.93	2.333	347.164	10.847	751.94	2.458	385.153	5.407	705.52	2.734
300.189	13.833	797.40	2.200	326.159	15.543	775.86	2.318	348.176	11.609	751.87	2.482	386.162	6.068	705.46	2.741
301.167	14.645	797.32	2.199	327.173	16.382	775.78	2.312	349.156	12.349	751.81	2.463	387.165	6.725	705.40	2.717
302.182	15.483	797.25	2.203	328.165	17.206	775.71	2.318	350.160	13.103	751.74	2.482	388.153	7.367	705.34	2.709
303.188	16.310	797.17	2.205	329.179	18.039	775.63	2.329	351.157	13.855	751.67	2.475	389.165	8.031	705.28	2.718
304.155	17.109	797.10	2.196	330.184	18.868	775.56	2.323	352.172	14.623	751.60	2.507	390.159	8.690	705.22	2.733
305.153	17.931	797.02	2.223	331.154	19.669	775.49									
0.29452 H ₂ O + 0.70548 CH ₃ OH															
282.525	4.316	879.57		304.188	10.295	864.36	2.481	341.168	12.965	832.86	2.625	365.170	15.942	817.23	2.697
283.170	4.351	879.55		305.158	11.322	864.27	2.480	342.159	13.920	832.78	2.637	366.160	16.856	817.15	2.705
284.161	5.379	879.46		306.164	12.384	864.17	2.485	343.179	14.907	832.69	2.636	367.169	17.815	817.07	2.706
285.189	6.499	879.36		307.164	13.436	864.08	2.502	344.182	15.888	832.61	2.641	368.175	18.760	816.99	2.709
286.255	7.660	879.26	2.415	308.163	14.491	863.99	2.511	345.154	16.838	832.53	2.644	369.165	19.697	816.91	2.708
287.176	8.703	879.17	2.419	309.154	15.542	863.90	2.516	346.151	17.808	832.44	2.646	369.530	4.434	804.05	
288.159	9.812	879.08	2.418	310.175	16.624	863.81	2.526	347.178	18.812	832.36	2.648	370.161	5.002	804.00	2.715
289.153	10.921	878.98		311.155	17.659	863.72	2.532	348.165	19.778	832.28	2.654	371.177	5.892	803.93	2.720
290.166	12.046	878.89	2.426	312.168	18.736	863.63	2.536	350.155	2.025	818.41	2.657	372.169	6.712	803.86	2.718
291.179	13.197	878.79		313.179	19.802	863.54	2.545	351.157	2.924	818.34	2.665	373.179	7.623	803.78	2.728
292.185	14.306	878.70	2.416	314.186	20.870	863.44	2.544	352.158	3.849	818.26	2.659	374.150	8.498	803.71	2.704
293.152	15.385	878.61	2.407	329.468	1.666	833.84		353.155	4.760	818.18	2.669	375.154	9.395	803.64	2.714
294.157	16.496	878.52	2.418	330.161	2.334	833.78		354.181	5.708	818.10	2.672	376.154	10.286	803.56	2.748
295.163	17.612	878.42	2.436	331.174	3.311	833.70	2.574	355.167	6.617	818.03	2.679	377.152	11.189	803.48	2.713
296.159	18.718	878.33	2.441	332.171	4.272	833.61	2.592	356.177	7.553	817.95	2.678	378.176	12.125	803.40	2.754
297.154	19.821	878.24	2.452	333.162	5.223	833.53	2.593	357.160	8.460	817.86	2.677	379.168	13.016	803.33	2.738
297.240	3.216	864.97		334.175	6.207	833.45	2.594	358.169	9.399	817.79	2.674	380.154	13.907	803.26	2.756
298.179	3.976	864.90		335.167	7.159	833.36	2.599	359.171	10.336	817.71	2.685	381.163	14.817	803.18	2.733
299.171	4.938	864.81		336.183	8.144	833.28	2.605	360.168	11.273	817.63	2.687	382.160	15.721	803.10	2.773
300.165	6.006	864.73		337.163	9.087	833.20	2.614	361.179	12.220	817.55	2.690	383.176	16.647	803.02	2.765
301.156	7.062	864.64		338.176	10.067	833.11	2.616	362.151	13.126	817.47	2.693	384.162	17.527	802.95	2.778
302.178	8.150	864.54	2.456	339.180	11.042	833.03	2.627	363.155	14.061	817.39	2.694	385.157	18.415	802.87	2.750
303.167	9.207	864.45		340.178	12.010	832.94	2.628	364.150	14.987	817.31	2.692	386.153	19.313	802.79	2.766
0.76649 H ₂ O + 0.23351 CH ₃ OH															
340.172	8.877	919.80	3.362	362.181	4.870	898.89	3.117	373.174	20.020	897.80	2.966	383.177	14.046	885.95	2.859
341.200	9.787	919.65	3.354	363.151	6.228	898.78	3.117	374.156	21.386	897.72	2.940	384.158	15.427	885.85	2.815
342.160	10.906	919.50	3.318	364.153	7.604	898.67	3.078	375.240	3.712	886.72		385.156	16.791	885.76	2.861
343.158	12.127	919.36	3.306	365.172	8.999	898.57	3.092	376.169	5.063	886.62		386.155	18.167	885.67	2.855
344.157	13.371	919.23	3.281	366.156	10.350	898.47	3.064	377.176	6.426	886.52	2.940	387.160	19.550	885.57	2.851
345.152	14.612	919.12	3.236	367.162	11.730	898.36	3.079	378.171	7.587	886.41	2.938	388.159	20.921	885.48	2.822
346.165	15.877	919.01	3.262	368.159	13.104	898.27	3.073	379.160	8.913	886.30	2.923	390.220	2.165	872.39	2.729
347.169	17.148	918.90	3.247	369.154	14.476	898.17	3.038	380.169	10.274	886.20	2.926	391.153	3.360	872.30	2.710
348.163	18.402	918.80	3.215	370.171	15.878	898.07	2.992	381.164	11.621	886.10	2.862	392.164	4.795	872.19	2.668
349.154	19.651	918.70	3.209	371.176	17.264	897.98	2.996	382.168	12.992	886.00	2.880	393.177	6.175	872.08	2.662
350.177	20.928	918.61	3.197	372.178	18.644	897.89	2.995								

^a In K. ^b In MPa. ^c In kg·m⁻³. ^d In J·g⁻¹·K⁻¹.

temperature profile would be very large compared to that for the volume, the effect is not as large on the results.

For example, if the actual temperature of a volume is 30 K higher than the assumed temperature profile, the density

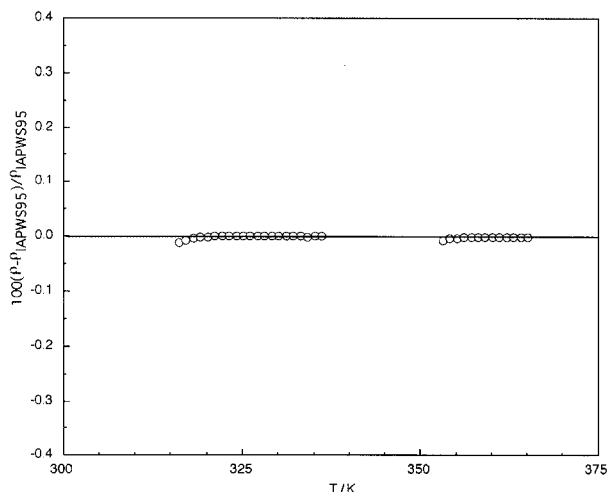


Figure 3. Deviations of measured densities for H₂O from calculations with IAPWS-95.¹⁶

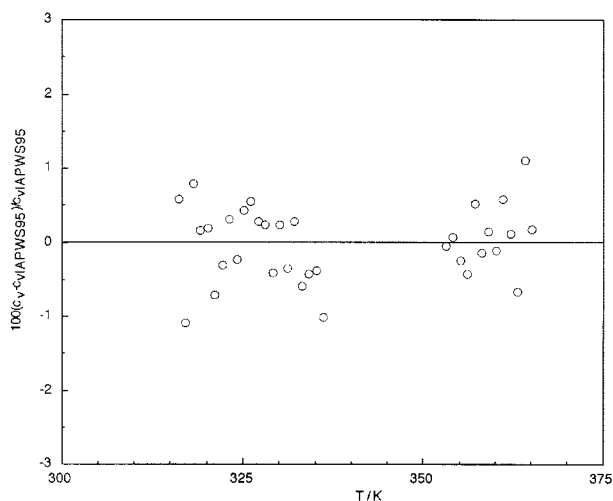


Figure 4. Deviations of measured c_v for H₂O from calculations with IAPWS-95.¹⁶

decreases about 1%, leading to an ~ 8 mg error of the sample mass. This amount can be compared with the 0.2 mg expanded uncertainty of the mass measurement, based on the balance's specifications. Thus, the estimated expanded relative uncertainty for the density measurement is 0.2%.

Figure 3 shows the deviations of experimental densities of H₂O from those calculated with the IAPWS-95 formulation.¹⁶ Deviations from this international reference equation of state were not greater than 0.01%. The uncertainty of the noxious volume of 2% propagates to a 0.03% uncertainty in the density values for this apparatus. To improve the accuracy of the density measurement, a more precise measurement of the noxious volume would be needed. Also, unphysical behavior at the lowest pressures was observed, due to less reliable pressure measurements at pressures below 10% of the full-scale range (68 MPa) of the pressure transducer. To improve this situation, a second pressure transducer with a lower full-scale range would be needed.

Figure 4 shows a comparison of the calculated c_v of H₂O with the IAPWS-95 formulation. The plot shows that deviations of c_v are within $\pm 1\%$. While 1% is a reasonable deviation, we would expect deviations to improve if this series were repeated, since the series depicted in Figure 4 had occasional problems with temperature excursions of

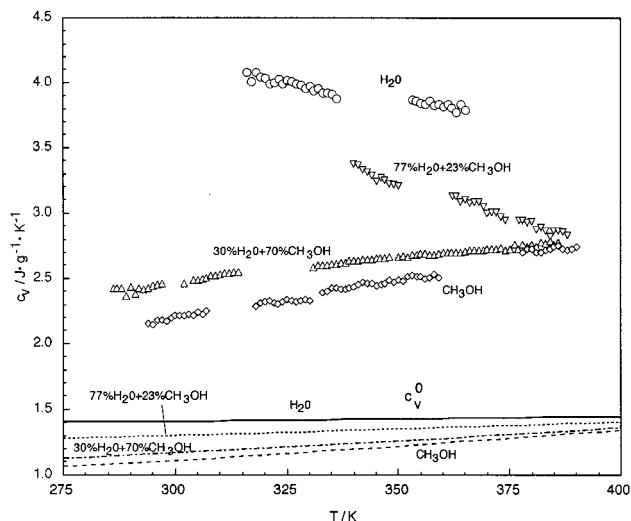


Figure 5. Measurements of c_v for H₂O, CH₃OH, 0.29452 H₂O + 0.70548 CH₃OH, and 0.76649 H₂O + 0.23351 CH₃OH as a function of temperature; ideal gas c_v^0 curves are shown for comparisons.

the adiabatic shields. Future results are expected to be more accurate because of optimization of the control. The measured data of H₂O were also compared with IAPWS-IF97,¹⁷ but the differences were negligible, as expected. It was found that densities and heat capacities calculated with IAPWS-95 differ by less than 0.0015% and 0.076%, respectively, from those calculated with IAPWS-IF97.

For CH₃OH, an equation of state¹⁸ has been formulated and published under IUPAC auspices. The measured results for CH₃OH were compared with the equation of state. The measured densities differed from the calculation within $\pm 0.1\%$. However, the measured heat capacities deviated by between +1.8% and +4.5% from the equation of state. This is considerably more than the uncertainty of the measurements. The main reason for the discrepancy seems to be that the equation was formulated without any experimental information for heat capacity in the liquid region.

Figure 5 depicts the c_v data of H₂O, CH₃OH, and their mixtures. Ideal heat capacities c_v^0 , which were calculated with published correlations^{16,18} and ideal mixing rules, are superimposed on this figure. The figure shows a remarkable composition-dependent behavior of the thermodynamic surface for the H₂O + CH₃OH binary system. While the ideal gas curves, the methanol-rich mixture curve, and the pure methanol curve increase slowly with temperature, the water-rich mixture curve and pure water curve decrease with temperature. One could readily guess that a mixture composition exists, between those measured, for which the liquid heat capacities are nearly independent of temperature in this region. Finally, the measurements reported in this work are of adequate accuracy for model tests, but were measured primarily for the purpose of performance tests of the new apparatus. Later measurements will incorporate improved temperature control of the shields and are expected to have lower uncertainty.

Acknowledgment

The authors gratefully acknowledge Katsumasa Araoka and his group of PIC, Toshiba Corporation, for his design and their construction of the twin-cell adiabatic calorimeter. We also thank Hidehiko Ichikawa of Sanyo Electric Software Co., Ltd. for his technical assistance.

Literature Cited

- (1) D'Arrigo, G.; Paparelli, A. Anomalous Ultrasonic Absorption in Alkoxyethanols Aqueous Solutions near their Critical and Melting Points. *J. Chem. Phys.* **1989**, *91*, 2587–2593.
- (2) Kubota, H.; Tanaka, Y.; Makita, T. Volumetric Behavior of Pure Alcohol and their Water Mixtures under High Pressures. *Int. J. Thermophys.* **1987**, *8*, 47–70.
- (3) Osada, O.; Sato, M.; Uematsu, M. Thermodynamic Properties of $\{x\text{CH}_3\text{OH}+(1-x)\text{H}_2\text{O}\}$ with $x = (1.000 \text{ and } 0.4993)$ in the Temperature Range from 320 K to 420 K at Pressures up to 200 MPa. *J. Chem. Thermodyn.* **1999**, *31*, 451–464.
- (4) Xiao, C.; Bianchi, H.; Tremaine, P. R. Excess Molar Volume and Densities of (Methanol+Water) at Temperatures between 323 and 573 K and at Pressures of 7 MPa and 13.5 MPa. *J. Chem. Thermodyn.* **1997**, *29*, 261–286.
- (5) Lama, R. F.; Lu, B. C.-Y. Excess Thermodynamic Properties of Aqueous Alcohol Solutions. *J. Chem. Eng. Data* **1965**, *10*, 216–219.
- (6) Benson, G. C.; D'Arcy, P. J. Excess Isobaric Heat Capacities of Water–*n*-Alcohol Mixtures. *J. Chem. Eng. Data* **1982**, *27*, 439–442.
- (7) Simonson, J. M.; Bradley, D. J.; Busey, R. H. Excess Molar Enthalpies and the Thermodynamics of (Methanol+Water) to 573 K and 40 MPa. *J. Chem. Thermodyn.* **1987**, *19*, 479–492.
- (8) Abdulagatov, I. M.; Dvoryanchikov, V. I.; Aliev, M. M.; Kamalov, A. N. Isochoric Heat Capacity of a 0.5 Water and 0.5 Methanol Mixture at Subcritical and Supercritical Conditions. *Steam, Water, and Hydrothermal Systems: Physics and Chemistry Meeting the Needs of Industry, Proceedings of the 13th International Conference on the Properties of Water and Steam*; Tremaine, P. R., Hill, P. G., Irish, D. E., Balakrishnan, P. V., Eds.; NRC Press: Ottawa, 2000; pp 157–164.
- (9) Hemminger, W.; Hohne, G. *Calorimetry—Fundamentals and Practice*; Verlag Chemie: Weinheim, 1984.
- (10) Magee, J. W. High-Temperature Adiabatic Calorimeter for Constant-Volume Heat Capacity Measurements of Compressed Gases and Liquids. *Proceedings of the 9th Symposium on Energy and Engineering Sciences*; Argonne National Laboratory, NTIS: Springfield, VA, 1991; pp 318–322.
- (11) Magee, J. W.; Blanco, J. C.; Deal, R. J. High-Temperature Adiabatic Calorimeter for Constant-Volume Heat Capacity of Compressed Gases and Liquids. *J. Res. Natl. Inst. Stand. Technol.* **1998**, *103*, 63–75.
- (12) Magee, J. W.; Kagawa, N. Specific Heat Capacity at Constant Volume for $\{x\text{NH}_3+(1-x)\text{H}_2\text{O}\}$ at Temperatures from 300 to 520 K and Pressures to 20 MPa. *J. Chem. Eng. Data* **1999**, *43*, 1082–1090.
- (13) Kuroki, T.; Kagawa, N.; Araoka, K.; Endo, H.; Tsuruno, S. Specific Heat Capacity Measurement of Fluids with an Adiabatic Calorimeter. *Proceedings of the 20th Japanese Symposium on Thermophysical Properties*, Tokyo, Japanese Society of Thermophysical Properties: Atsugi, Kanagawa, 1999; pp 456–460.
- (14) Goodwin, R. D.; Weber, L. A. Specific Heats C_v of Fluid Oxygen from the Triple Point to 300 K at Pressures to 350 Atmospheres. *J. Res. Natl. Bur. Stand. (U.S.)* **1969**, *73A*, 15–24.
- (15) *JSME Data Book: Heat Transfer*, 4th ed.; JSME: Tokyo, 1994.
- (16) Wagner, W.; Pruß, A. New International Formulation for the Thermodynamic Properties of Ordinary Water Substance for General and Scientific Use. *J. Phys. Chem. Ref. Data* (to be submitted).
- (17) Wagner, W.; Cooper, J. R.; Dittmann, A.; Kijima, J.; Kretschmar, H.-J.; Kruse, A.; Mares, R.; Oguchi, K.; Sato, H.; Stocker, I.; Sifner, O.; Takaishi, Y.; Tanishita, I.; Trubenbach, J.; Willkommen, Th. The IAPWS Industrial Formulation 1997 for the Thermodynamic Properties of Water and Steam. *ASME J. Eng. Gas Turbines Power* **2000**, *122*, 150–182 (see also *IAPWS Release on the IAPWS Industrial Formulation 1997 for the Thermodynamic Properties of Water and Steam*, 1997; pp 1–48.)
- (18) de Reuck, K. M.; Craven, R. J. B. *Methanol—International Thermodynamic Tables of the Fluid State—12*; Blackwell: Oxford, 1993.

Received for review August 4, 2000. Accepted May 14, 2001.

JE0002437